Published OnlineFirst June 25, 2015; DOI: 10.1158/0008-5472.CAN-15-0129

Cancer Research

A Polymer-Based Antibody–Vinca Drug Conjugate Platform: Characterization and Preclinical Efficacy

Alexander V. Yurkovetskiy, Mao Yin, Natalya Bodyak, Cheri A. Stevenson, Joshua D. Thomas, Charles E. Hammond, LiuLiang Qin, Bangmin Zhu, Dmitry R. Gumerov, Elena Ter-Ovanesyan, Alex Uttard, and Timothy B. Lowinger

Abstract

Antibody–drug conjugates (ADC) are an emerging drug class that uses antibodies to improve cytotoxic drug targeting for cancer treatment. ADCs in current clinical trials achieve a compromise between potency and physicochemical/pharmacokinetic properties by conjugating potent cytotoxins directly to an antibody at a 4:1 or less stoichiometric ratio. Herein, we report a novel, polyacetal polymer-based platform for creating ADC that use poly-1-hydroxymethylethylene hydroxymethylformal (PHF), also known as Fleximer. The high hydrophilicity and polyvalency properties of the Fleximer polymer can be used to produce ADC with high drug loading without compromising physicochemical and pharmacokinetic properties. Using trastuzumab and a vinca drug derivative to demonstrate the utility of this platform, a novel Fleximer-based ADC was prepared and characterized *in vivo*. The ADC prepared had a vinca-antibody ratio of 20:1. It exhibited a high antigen-binding affinity, an excellent pharmacokinetic profile and antigen-dependent efficacy, and tumor accumulation in multiple tumor xenograft models. Our findings illustrate the robust utility of the Fleximer platform as a highly differentiated alternative to the conjugation platforms used to create ADC currently in clinical development. *Cancer Res; 75(16); 1–8. ©2015 AACR.*

Introduction

Antibody–drug conjugates (ADC) represent a unique and emerging drug class that relies on monoclonal antibody (mAb) recognition of specific cancer-associated antigens for targeted delivery of chemotherapeutic agents. mAb-directed drug delivery can provide significant advantages over traditional chemotherapy, which often yields systemic toxicities, and unconjugated mAb therapy, which often suffers from limited clinical efficacy (1). The recent success of two FDA-approved ADCs, brentuximab vedotin (2) and trastuzumab emtansine (3), has established the clinical effectiveness of this drug class. ADCs have yet to reach their full potential as anticancer therapeutics, and active research on the design of efficacious and well-tolerated ADCs continues to provide insight into the choice of target antigen, ADC stability and pharmacokinetics (PK), linker chemistries, methods of conjugation, and choice of drug payload (1, 4).

Early approaches to ADC design logically centered on the use of clinically validated chemotherapeutic agents as payloads for attachment to mAbs. These first-generation ADCs exhibited preclinical promise using established drugs, such as vinblastine (5), doxorubicin (6), and methotrexate (7). However, these ADCs met with limited success in the clinic where the therapeutic index was poor and high doses were often required to demonstrate antitumor activity (6, 7).

With the aim of improving the efficacy of ADCs, second-generation approaches increased potency by replacing clinically validated drugs, such as vinblastine and doxorubicin, with auristatin or maytansine derivatives, cytotoxic agents that are 100- to 1,000-fold more toxic *in vitro* (4, 8). Extensive work by scientists at Seattle Genetics (9, 10) and ImmunoGen (11) demonstrated the viability of these more potent cytotoxins as ADC payloads, and studies on the stoichiometry of drug loading revealed that the *in vitro* potency of ADCs is dependent on the drug to antibody ratio (DAR; ref. 9). Although a higher DAR is associated with increased *in vitro* potency, it also has detrimental effects on the properties of ADCs. Increased drug content negatively affects the pharmacokinetic properties of the ADC (9), and because drug payloads are highly hydrophobic, an increase in DAR yields ADCs that are prone to aggregation (12). Ultimately, a compromise between potency and *in vivo* properties was reached with an average DAR of 4, which provided the best antitumor activity (8, 9).

Herein, we describe a novel polyacetal polymer-based ADC platform using poly-1-hydroxymethylethylene hydroxymethylformal (PHF), also known as Fleximer. The high hydrophilicity and polyvalency properties of the Fleximer polymer can be used to overcome the limitations of direct drug–antibody conjugation, permitting high drug loading with a variety of payloads without compromising the physicochemical and pharmacokinetic properties of the ADC. Typical direct drug–antibody conjugated ADCs contain 3 to 4 highly potent cytotoxins/mAb. In this report, we demonstrate the efficacy of a Fleximer-based ADC that uses

Mersana Therapeutics, Inc., Cambridge, Massachusetts.

Note: Supplementary data for this article are available at Cancer Research Online (http://cancerres.aacrjournals.org/).

Corresponding Author: Timothy B. Lowinger, Mersana Therapeutics, Inc., 840 Memorial Drive, Cambridge, MA 02139. Phone: 617-498-0020; Fax: 617-498-0109; E-mail: tlowinger@mersana.com

doi: 10.1158/0008-5472.CAN-15-0129

Published OnlineFirst June 25, 2015; DOI: 10.1158/0008-5472.CAN-15-0129

trastuzumab as the targeting moiety and a modestly potent vinca derivative as the cytotoxic payload. An ester-based linker is used to conjugate the vinca payload to the polymer backbone, which in turn is conjugated to the antibody via hinge-region cysteine residues. The resultant Fleximer-based ADC is observed to be highly stable in circulation, and it is presumed that, upon antigen binding and internalization, processing of the ADC to release free vinca can occur by a combination of processes, including catabolism of the antibody (13), pH-dependent hydrolysis of the polyacetal polymer backbone (14), and carboxyesterase cleavage of the linker ester bond (15). This novel ADC, with a DAR of 20, maintains excellent physicochemical properties and demonstrates sub-nanomolar potency *in vitro* and target-dependent accumulation and efficacy in *in vivo* models of human breast and gastric cancers.

Materials and Methods

Monoclonal antibodies

Trastuzumab (herceptin) and rituximab were purchased from Myoderm.

Preparation of Fleximer ADCs

Fleximer ADCs were prepared by conjugation of IgG_1 mAbs (trastuzumab or rituximab) to the Fleximer vinca conjugate according to the following procedures.

N-(3-hydroxypropyl)vindesine (HPV, I). HPV (free vinca) was prepared from vinblastine sulfate as previously described (16). HPV was isolated as a trifluoroacetate salt with >95% purity using HPLC.

N-(3-hydroxypropyl)vindesine alanine (HPV-Ala-NH_2, II). See Supplementary Fig. S1 for schematic of HPV-Ala-NH_2 synthesis. Boc-L-alanine (0.681 g, 3.60 mmol) and N,N′-diisopropylcarbodiimide (DIC; 0.561 mL, 3.60 mmol) were combined in dichloromethane (DCM; 15 mL) at 0°C and stirred for 15 minutes. In a separate flask, HPV (1.462 g, 1.800 mmol) and 4-N,N-dimethylaminopyridine (DMAP; 0.660 g, 5.40 mmol) were dissolved in DCM (15 mL) at 0°C. The reagent solutions were combined and stirred at 0°C for 1 hour, brought to room temperature and stirred for an additional 2 hours. The resulting solution was diluted with DCM (50 mL), washed with water, and extracted (2x) with aqueous citric acid (1% w/v). The combined citric acid washes were treated with solid sodium bicarbonate, extracted with DCM, dried over sodium sulfate, and vacuum concentrated. Crude HPV-Boc-alanine (1.4 g) was dissolved in DCM (55 mL) and treated with trifluoroacetic acid (TFA; 5.5 mL) at 0°C for 1 hour. Following solvent evaporation, the crude product was dissolved in DMSO and purified by preparative reversed-phase HPLC. Lyophilization of product-containing fractions yielded HPV-Ala-NH_2 trifluoroacetate salt as an off-white amorphous solid [59% yield; HPLC purity 96%; MS (ESI+) m/z: 883.4 (M+1)]. ^{1}H-NMR was consistent with the expected structure.

See Fig. 1 for schematic of the multistep synthesis of trastuzumab–PHF–vinca (PHF-GA-(Ala-HPV) trastuzumab).

Poly-1-hydroxymethylethylene hydroxymethyl-formal (III). The Fleximer polymer backbone, PHF, was prepared as previously described (14, 17, 18).

PHF-glutaric acid (PHF-GA, IV). 4-N,N-Dimethylaminopyridine (0.268 g, 2.91 mmol) and glutaric anhydride (1.375 g, 12.06 mmol) were added to a solution of PHF (MW ∼10 kDa; 1.48 g, 10.96 mmol PHF structural unit) in dimethylacetamide (DMA; 300 mL) and anhydrous pyridine (33.3 mL). The reaction mixture was stirred at 60°C for 18 hours. Solvents were removed under reduced pressure and the resulting thick oil was dissolved in water (100 mL). The pH was adjusted to 6.0 to 6.5 with 5N NaOH. The resulting clear solution was diluted to 200 mL with water, filtered through a 0.2-μm filter, and purified by diafiltration using a membrane filter (3-kDa MWCO). Water was removed by lyophilization yielding PHF-GA as a white solid (1.28 g; 48% yield). Twenty-five percent of total PHF monomer units were substituted with glutaric acid, as determined by ^{1}H-NMR. ^{1}H-NMR (D_2O): 4.85 ppm (m, 1H, acetal, PHF); 4.4–3.5 ppm (mm, 7H, methylene and methyne protons, PHF); 2.5 ppm (bt, 2H, α-methylene protons, GA); 2.35 ppm (bt, 2H, γ-methylene, GA); and 1.9 ppm (bt, 2H, β-methylene protons, GA).

Pyridyl disulfide (SSPγ)-modified PHF-GA (PHF-GA-SSPγ, V). PHF-GA (1.63 g, 11.12 mmol) was dissolved in water (10 mL) and N-hydroxysuccinimide (NHS; 0.154 g, 1.33 mmol) was added. The mixture was cooled to 0°C and an aqueous solution of 1-ethyl-3-[3-dimethylaminopropyl]carbodiimide hydrochloride (EDC; 0.256 g, 1.33 mmol) was added, followed by 2-(pyridine-2-yldisulfanyl)ethaneamine hydrochloride (0.297 g, 1.33 mmol). The pH was adjusted to 5.5–6.0 and the mixture was stirred at room temperature for 18 hours. PHF-GA-SSPy was purified by diafiltration and lyophilized to a white solid (1.66 g; 86% yield). The SSPy group content was 3% mol relative to PHF monomer units, as determined by spectrophotometry. ^{1}H-NMR (D_2O): 8.45 ppm (bs, 1H, Ar, Py); 7.9 ppm (bs, 2H, Ar, Py); 7.35 ppm (bs, 1H, Ar, Py); 4.9 ppm (m, 1H, acetal, PHF); 4.4–3.6 ppm (m, 7H, methylene and methyne protons, PHF); 3.3–2.8 ppm (m, 4H, methylene protons, cysteamine linker); 2.5 ppm (bt, 2H, α-methylene protons, GA); 2.3 ppm (bt, 2H, γ-methylene, GA); 2.0–1.9 ppm (bt, 2H, β-methylene protons, GA).

PHF-GA-(SH)-(Ala-HPV; PHF-vinca, VI). PHF-GA-SSPy (289.0 mg, 0.023 mmol) was dissolved in water (8 mL) and acetonitrile (4 mL) and cooled to 0°C. NHS (26.4 mg, 0.230 mmol) was added, followed by an aqueous solution of EDC (44.0 mg, 0.230 mmol) and HPV-Ala-NH_2 (131.45 mg, 0.138 mmol). The pH of the resulting mixture was adjusted to 6.0, and the solution was stirred at room temperature overnight. The pH was adjusted to 7.5 with 1 mol/L sodium bicarbonate, and dithiothreitol (DTT; 37.8 mg, 0.245 mmol) was added. The reaction mixture was stirred for 30 minutes, diluted to 15 mL with water, and PHF-vinca (Fleximer vinca conjugate) was purified by diafiltration (57% yield, HPV-based). The HPV content was 7.3% wt, as determined by spectrophotometry. ^{1}H-NMR (D_2O): Product spectrum showed characteristic signals of aromatic protons of HPV at 7.65, 7.45, 7.20, 6.6, 6.45, 6.0, and 5.8 ppm; signals of HPV methyl and methylene protons at 0.8–1.8 ppm; and signals of PHF-GA at 1.9–4.8 ppm.

Trastuzumab-MCC (VII). Trastuzumab (10 mg) was diluted in PBS pH 7.0 (1 mL), and then a solution of succinimidyl-4-(N-maleimidomethyl)cyclohexane-1-carboxylate (SMCC) in DMSO (5 μL, 30 mg/mL) was added. The resulting solution was stirred at room temperature for 2 hours. Trastuzumab-MCC was purified by gel filtration on a Sephadex G-25 column equilibrated with PBS

Published OnlineFirst June 25, 2015; DOI: 10.1158/0008-5472.CAN-15-0129

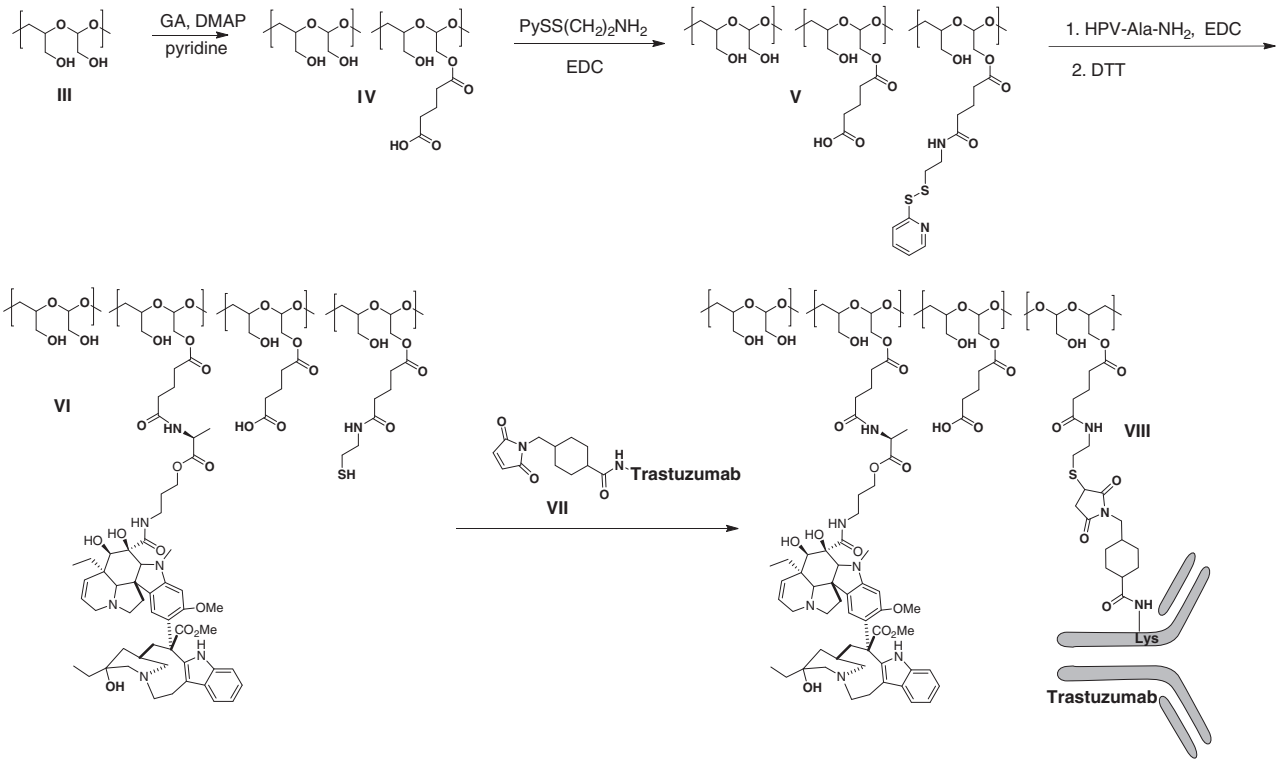

Figure 1.
Synthesis of trastuzumab–PHF–vinca ADCs.

(90% yield). An average of 5 to 6 maleimido groups were linked to each trastuzumab molecule, as determined by spectrophotometry (280/320 nm).

Rituximab-MCC. Rituximab-MCC was prepared in a manner analogous to that described for trastuzumab-MCC.

PHF-GA-(Ala-HPV) trastuzumab (trastuzumab–PHF–vinca, VIII). PHF-GA-(SH)-(Ala-HPV; 11.2 mg) in water (0.5 mL) was added to trastuzumab-MCC (20 mg) in PBS pH 7.0 (2 mL). The solution was stirred at room temperature for 4 hours. The resulting trastuzumab–PHF–vinca conjugate was purified by gel filtration on a Superose 6 column equilibrated with PBS and concentrated using a membrane filter (10-kDa MWCO; 75% yield, protein-based). The DAR was 20, as determined by spectrophotometry (the extinction coefficients for HPV at 280 nm and 310 nm are 17,640 per mol/cm and 7,259 per mol/cm, respectively). The MW of the ADC was approximately 170 kDa, as determined by SEC relative to protein standards.

PHF-GA-(Ala-HPV) rituximab (rituximab–PHF–vinca). Rituximab–PHF–vinca was prepared using rituximab-MCC in a manner analogous to that described for trastuzumab–PHF–vinca.

Determination of binding affinity using surface plasmon resonance

Surface plasmon resonance (SPR) was used to estimate the binding affinity of trastuzumab–PHF–vinca to antigen in direct comparison with that of trastuzumab under identical conditions over the same surface. Binding studies were performed by Xtal BioStructures Inc. using a Bio-Rad ProteOn XPR36 optical biosensor with GLC sensor chip equilibrated with running buffer (10 mmol/L HEPES, 150 mmol/L NaCl, 0.01% Tween-20, 0.2 mg/mL BSA, pH 7.4). Recombinant human Her2 protein was immobilized in flow channels using standard amine-coupling chemistry to densities of 420 and 1,320 response units. Binding studies were performed at 25°C. Trastuzumab–PHF–vinca samples were tested in a 3-fold dilution series starting at 27 nmol/L. Each concentration series was injected across the Her2 surfaces at 50 μL/minute for 8 minutes and dissociation was monitored for 1 hour. Surfaces were regenerated with three 30-second injections of 30 mmol/L H_3PO_4. The corresponding sensorgrams are provided in Supplementary Fig. S2 and S3.

Cell culture

Human breast cancer cell lines (BT-474, SK-BR-3, and MCF7) and the human gastric cancer cell line (NCI-N87) were purchased from the ATCC. Cell lines were used without further authentication. NCI-N87 cells were cultured according to recommended specifications; BT-474, SK-BR-3, and MCF7 cells were cultured in DMEM medium supplemented with 10% FBS and penicillin/streptomycin. All cell lines were maintained in a humidified incubator at 37°C, 5% CO_2.

Cell proliferation assay

The CellTiter-Glo Luminescent Cell Viability Assay (Promega) was used to obtain the IC_{50} values for trastuzumab–PHF–vinca, PHF-vinca, and HPV. Cells were seeded into 96-well plates at a density of 5×10^3 cells per well. Following overnight incubation, cells were treated with the test compounds at various

Published OnlineFirst June 25, 2015; DOI: 10.1158/0008-5472.CAN-15-0129

concentrations and incubated continuously for 72 hours. IC_{50} values are expressed as nmol/L HPV equivalents.

In vivo xenograft models

In vivo studies using female 9 to 10-week-old CB.17 SCID mice were conducted at Charles River Laboratories (Piedmont Research Center) in accordance with the *Guide for Care and Use of Laboratory Animals*. To establish tumors, 1×10^7 NCI-N87 cells in 50% Matrigel or 1 mm^3 BT-474 tumor fragments were implanted s.c. into the flank of each mouse. Tumor size was measured using calipers and tumor volume ($l \times w^2/2$) was determined, where l (mm) is the longest and w (mm) the shortest dimension of the tumor. Tumors were allowed to grow to a target range of 100 to 150 mm^3 before treatment was initiated. Mice received i.v. bolus injections of ADCs once a week for 3 weeks; a special treatment group received a single dose of ADCs. Mice injected with saline were used as vehicle control. To assess the effect of trastuzumab–PHF–vinca on large, well-established tumors, BT-474 xenografts were allowed to grow to a volume of about 350 mm^3 before treatment. Time-to-endpoint (TTE) was calculated for each mouse, and treatment response was determined from the percentage of tumor growth delay (TGD), defined as the percentage increase in the median TTE in treated mice versus the designated untreated controls. Body weight and other toxicity symptoms were monitored. Mice were sacrificed when tumor volume exceeded 700 mm^3 (NCI-N87 model) and either 800 or 1,000 mm^3 (BT-474 model).

Statistical analysis

For *in vivo* xenograft experiments, statistical analysis was performed by the log-rank and Mann–Whitney tests using Prism v3.03 (GraphPad Software).

Plasma pharmacokinetics

NCI-N87 tumor-bearing SCID mice were used for plasma pharmacokinetic studies. Mice received i.v. bolus injections of test compounds. Plasma samples were collected at 5 minutes and 24, 48, 72, and 168 hours ($n = 3$). Conjugated and free HPV were quantified by qualified LC/MS-MS assays following methods previously described (19). Total trastuzumab was quantified using a human IgG ELISA (Innovative Research) following the manufacturer's instructions. PK was examined by noncompartmental analysis using WinNonlin v5.2.1 (Pharsight Corporation).

Determination of total HPV in tumor tissue

BT-474 tumor-bearing SCID mice were used for tumor accumulation studies. Mice received i.v. bolus injections of test compounds. Tumor homogenate samples were analyzed using LC/MS-MS as previously described (19). Briefly, tumor homogenates were hydrolyzed under basic conditions (pH > 10) and the released HPV was extracted. The lower limit of quantification for the HPV assay was 20 ng/g.

Results

Antigen binding

To ascertain whether the conjugation of PHF–vinca to random lysine residues of the antibody had any impact on antigen affinity, the binding affinity of trastuzumab–PHF–vinca was compared with that of trastuzumab alone (Table 1). Because of the possibility of bivalent binding, as well as the limitations of accurately measuring very slow dissociation rates (k_{off}), the K_d and k_{off} values are considered apparent values. Under identical conditions, trastuzumab–PHF–vinca retained affinity comparable with the unconjugated trastuzumab antibody alone.

Cytotoxic activity of trastuzumab–PHF–vinca

The *in vitro* cytotoxicity of trastuzumab–PHF–vinca was assessed in Her2-positive and Her2-negative cell lines. Unconjugated PHF–vinca and the small-molecule vinca release product HPV were examined in parallel as controls (Table 2). All of the cell lines were susceptible to HPV in the low nanomolar range. Similarly, all cell lines were susceptible to PHF–vinca, albeit at approximately 10-fold higher concentrations. In contrast, trastuzumab–PHF–vinca inhibited the growth of the Her2 (3+) cell lines with low nanomolar potency and was significantly less active in the Her2 (0–1+) cell line.

Efficacy of Fleximer ADCs in a xenograft model of human gastric cancer

The *in vivo* antitumor activity of trastuzumab–PHF–vinca was first assessed in the Her2 (3+) NCI-N87 human gastric cancer xenograft model, in which the efficacy of ado-trastuzumab emtansine (T-DM1) has been reported (20). As shown in Fig. 2, tumor-bearing mice were treated with vehicle (saline control), trastuzumab alone (15.6 mg/kg antibody equivalents), PHF-vinca (1.2 mg/kg HPV equivalents), HPV (1.2 mg/kg), or trastuzumab–PHF–vinca. Two doses of trastuzumab–PHF–vinca were tested [15.6 mg/kg antibody equivalents (1.2 mg/kg HPV equivalents) and 5.2 mg/kg antibody equivalents (0.4 mg/kg HPV equivalents)]. Trastuzumab–PHF–vinca exhibited the greatest efficacy, with a 100% regression response rate (8 partial regressions and 2 complete regressions) on day 92 and a maximum TGD of 44.0 days (92%) at the 15.6 mg/kg dose. Treatment with 5.2 mg/kg of trastuzumab–PHF–vinca was also active, resulting in a TGD of 31.8 days (66%). Both dosages had significant survival benefit compared with vehicle ($P < 0.001$) and produced statistically significant tumor growth inhibition (TGI) that exceeded the potential therapeutic activity threshold. Trastuzumab alone was moderately active, providing a TGD of 12.3 days (26%), no regressions, and significant log-rank survival compared with vehicle ($P = 0.024$) with day 29 TGI of 67%. Treatment with either HPV or PHF–vinca did not yield significant antitumor activity. All treatments were well tolerated, with maximum mean body weight losses within acceptable limits for all groups. Clinical observations in all groups were unremarkable for potential treatment-related side effects.

Table 1. Her2-binding affinity[a]

Analyte	k_a (per mol/s) ($\times 10^5$)	k_d (per second) ($\times 10^{-6}$)	K_D (pmol/L)
Trastuzumab	7.152 ± 0.008	4 ± 1	6 ± 1
Trastuzumab–PHF–vinca ADC	4.426 ± 0.005	5.1 ± 0.7	12 ± 2

[a]Surface plasmon resonance measurements of human Her2 protein binding parameters at 25°C.

Published OnlineFirst June 25, 2015; DOI: 10.1158/0008-5472.CAN-15-0129

Table 2. IC_{50}[a] (nmol/L HPV equivalents) of fleximer ADCs

Cell line	Her2 expression	HPV (nmol/L)	PHF-vinca (nmol/L)	Trastuzumab–PHF–vinca ADC (nmol/L)
SK-BR-3	3+	1.8	20.1	1.3
BT-474	3+	0.8	8.3	0.8
NCI-N87	3+	4.3	46.4	6.9
MCF7	0–1+	3.6	56.3	73.7

[a]The IC_{50} value was determined by cell viability following 72-hour incubation with the indicated test compounds.

Efficacy of Fleximer ADCs in a xenograft model of human breast cancer

The antitumor activity of trastuzumab–PHF–vinca was further evaluated in the Her2 (3+) BT-474 human breast cancer xenograft model. Treatment with 7.5 mg/kg antibody equivalents of trastuzumab–PHF–vinca resulted in the maximum possible TGD with 100% tumor-free survivors on day 60 and day 14 TGI of 100% (Fig. 3). A single dose (20 mg/kg antibody equivalents) of this Fleximer ADC also produced the maximum TGD and 100% tumor-free survivors on day 60. In contrast, the non-binding control treatment, rituximab–PHF–vinca, produced only modest TGI with no partial or complete regressions. Trastuzumab alone was inactive, and trastuzumab in combination with unconjugated PHF–vinca resulted in very modest activity. All treatments were acceptably tolerated.

To assess the effect of tumor burden in this model as well as the efficacy of lower doses, a subsequent study was performed (Fig. 4). Dosing was initiated either when tumors reached a target range of 100 to 150 mm^3 or after tumors reached an average size of 344 mm^3 (individual tumor volumes ranged from 196 to 658 mm^3). Irrespective of initial tumor size, all trastuzumab–PHF–vinca dose groups resulted in a median TTE of 87 days, corresponding to the maximum achievable TGD (59.4 days, 215%), and 100% tumor-free survivors at the end of the study. At the completion of the study, the sites of tumor implantation in the higher tumor burden groups were excised, fixed in 10% formalin, embedded in paraffin, and sectioned. Hematoxylin and eosin staining revealed that small nodules in the subcutis had amorphous debris and extensive mineral deposits, some scar tissue, but no residual tumor cells (data not shown), establishing that all of the animals were tumor free.

Pharmacokinetics and tumor accumulation of Fleximer ADCs

The pharmacokinetic properties of trastuzumab–PHF–vinca were evaluated in SCID mice bearing NCI-N87 xenograft tumors after a single injection of 15 mg/kg antibody equivalents of trastuzumab–PHF–vinca (Fig. 5A). The plasma concentration of total trastuzumab was monitored by ELISA. Conjugated HPV and free HPV plasma concentrations were monitored by LC/MS-MS. The plasma concentrations of total trastuzumab and conjugated HPV showed a biphasic decline after the first 5-minute sampling time point with terminal elimination half-lives of approximately 9 and 3.5 days, respectively. Plasma exposure $AUC_{0\text{-inf}}$ to trastuzumab–PHF–vinca ADCs and conjugated HPV was 332 μg*day/mL and 26 μg*day/mL, respectively. The concentration of free HPV in plasma at all time points was lower than the detection limit of the assay (10 ng/mL), indicating that the plasma HPV concentration was at least 1,000-fold lower than that of conjugated HPV. PHF–vinca displayed rapid plasma elimination and was not detectable beyond the 24-hour time point.

Accumulation of total HPV (conjugated + free) following a single dose of trastuzumab–PHF–vinca (1.4 mg/kg HPV equivalents) or rituximab–PHF–vinca (1.4 mg/kg HPV equivalents) was evaluated in SCID mice bearing BT-474 xenograft tumors (Fig. 5B). Treatment with trastuzumab–PHF–vinca resulted in a 4-fold greater C_{max} and 9-fold greater $AUC_{0\text{-}t}$ for total HPV in tumors relative to treatment with the non-binding control ADC rituximab–PHF–vinca.

Discussion

The underlying concept of an ADC is both simple and elegant: To use the inherent specificity of an antibody to a tumor-associated antigen to selectively deliver a therapeutic payload to kill the tumor while sparing healthy tissues. One of the fundamental challenges in creating an effective ADC has been to covalently attach a sufficient number of drug payload molecules to the antibody to enable efficient accumulation of the drug in the tumor without significantly impairing the physicochemical and drug-like properties of the antibody. Consequently, the vast majority of ADCs in clinical development have a DAR of 4 or less and rely on highly potent cytotoxic molecules (1); there are

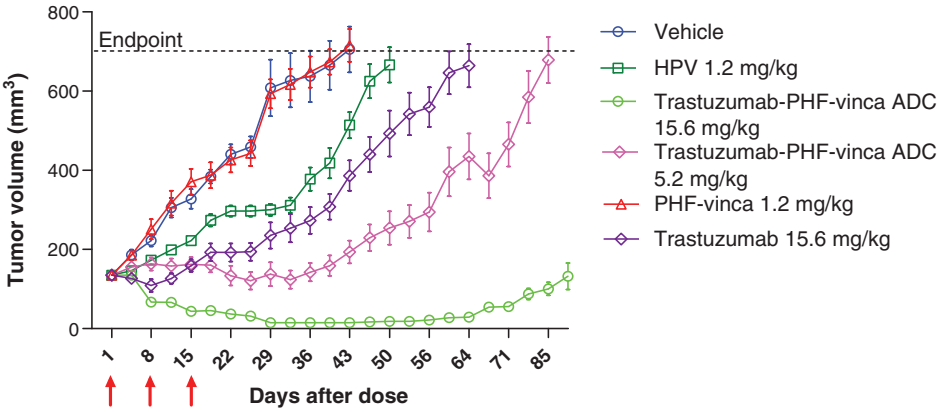

Figure 2.
Antitumor activity of Fleximer ADCs in an NCI-N87 xenograft model. Treatment was initiated 12 days following tumor cell implantation (designated as day 1). Mice ($n = 10$) received i.v. injections of tested material once per week for 3 weeks (qwk × 3) as indicated by arrows. The dose of Fleximer ADCs (trastuzumab–PHF–vinca ADC) is expressed in antibody equivalents. The dose of HPV (free vinca) and PHF-vinca (Fleximer vinca conjugate; expressed in toxin equivalents) was equal to the highest dose of Fleximer ADCs.

Published OnlineFirst June 25, 2015; DOI: 10.1158/0008-5472.CAN-15-0129

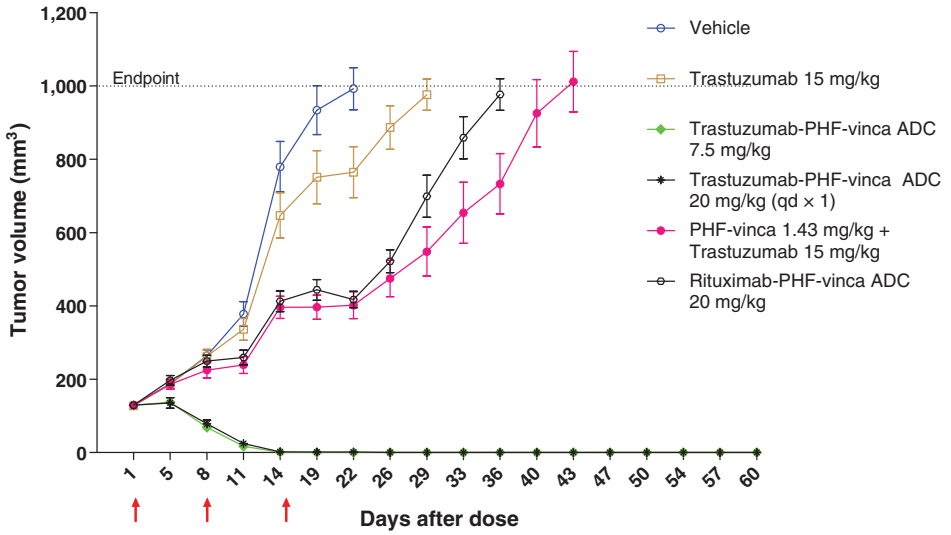

Figure 3.
Antitumor activity of Fleximer ADCs in a BT-474 xenograft model. Treatment was initiated 24 days following tumor fragment implantation (designated as day 1). Mice ($n = 12$) received i.v. injections of tested material once per week for 3 weeks (qwk × 3) as indicated by arrows. The dose of Fleximer ADCs (trastuzumab–PHF–vinca ADC) is expressed in antibody equivalents. Fleximer ADCs were also evaluated at a single dosage administered once on day 1 (qd × 1). The dose of PHF-vinca (Fleximer vinca conjugate; expressed in toxin equivalents) was equal to the highest dose of Fleximer ADCs.

only limited examples of ADCs using moderately cytotoxic drugs (21).

With the polymer approach to ADCs described herein, we demonstrate that significantly higher DARs can be achieved while maintaining excellent drug-like qualities of the resultant ADC. Furthermore, we demonstrate that a highly potent and efficacious ADC can be constructed using a moderately potent vinca derivative as the payload drug (low nanomolar potency compared with the sub-nanomolar potency of maytansines and auristatins).

For an ADC to selectively deliver drug to a tumor it must bind to its intended target, and it was unclear *a priori* whether the conjugation of PHF polymers to the antibody would negatively affect this essential property. As evidenced by antigen affinity measurements, trastuzumab–PHF–vinca ADCs with a DAR of 20 maintain excellent affinity for the Her2 antigen (Table 1). Furthermore, target-dependent cytotoxicity, a key ADC attribute, was maintained, as shown by the 10- to 75-fold lower potency of trastuzumab–PHF–vinca ADCs in the Her2 (0–1+) MCF7 cells relative to the Her2 (3+) cell lines (Table 2).

In contrast with potency *in vitro*, the efficacy of an ADC *in vivo* may also be influenced by a number of properties, including PK, tumor penetration, tumor accumulation, and duration of exposure. To this end, we characterized the properties of the trastuzumab–PHF–vinca ADC in two distinct Her2 (3+) xenograft models. In the NCI-N87 gastric tumor xenograft (Fig. 2), the trastuzumab–PHF–vinca ADC exhibits dose-dependent efficacy, with a 100% regression response rate (8 partial regressions and 2 complete regressions) and a maximum TGD of 44.0 days (92%) at the 15.6 mg/kg dose. Treatment with 5.2 mg/kg of trastuzumab–PHF–vinca was also active, resulting in a TGD of 31.8 days (66%). Treatment with trastuzumab alone was only modestly active at an equivalent dose, providing a TGD of 12.3 days (26%) and no regressions; thus, demonstrating the benefit of HPV conjugation to the antibody. Treatment with either HPV alone or PHF-vinca did not yield significant antitumor activity, further confirming the benefit of antibody conjugation.

It has been previously demonstrated that direct drug–antibody conjugation approaches yield an exposure *in vivo* (AUC) that is inversely proportional to drug loading (9). Our polymer-based

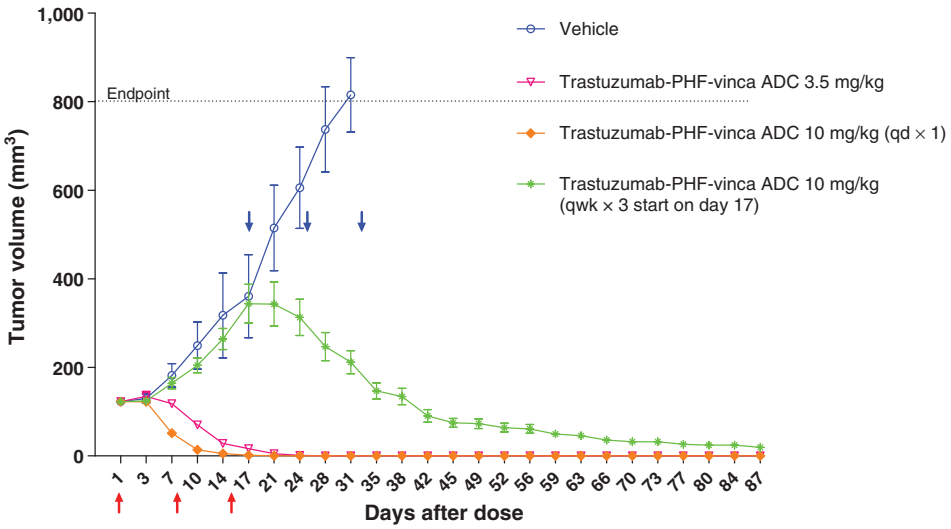

Figure 4.
Efficacy of Fleximer ADCs in a high tumor burden BT-474 xenograft model. In the low tumor burden model, treatment was initiated 21 days following tumor fragment implantation (mean tumor volume of 122 mm^3, designated as day 1). In the high tumor burden model, treatment was initiated on day 17 (mean tumor volume of 344 mm^3). Mice ($n = 10$) received i.v. injections of tested material once per week for 3 weeks (qwk × 3) as indicated by arrows. The dose of Fleximer ADCs (trastuzumab–PHF–vinca ADC) is expressed in antibody equivalents. Fleximer ADCs were also evaluated at a single dosage administered once on day 1 (qd × 1).

Published OnlineFirst June 25, 2015; DOI: 10.1158/0008-5472.CAN-15-0129

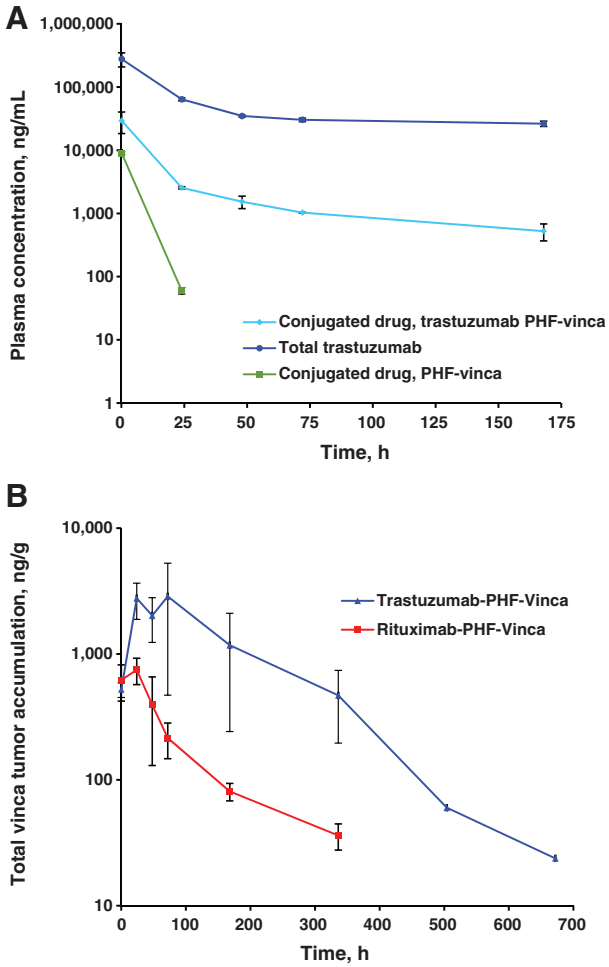

Figure 5.
Plasma PK of trastuzumab–PHF–vinca and tumor accumulation of total HPV in tumor-bearing mice. A, plasma PK of trastuzumab–PHF–vinca and PHF-vinca was determined in SCID mice ($n = 3$) bearing NCI-N87 xenograft tumors following a single i.v. injection of 15 mg/kg antibody equivalents or 1.4 mg/kg HPV equivalents, respectively. B, tumor accumulation of total HPV (conjugated + free) was determined in SCID mice ($n = 3$) bearing BT-474 xenograft tumors following a single i.v. injection of trastuzumab–PHF–vinca or rituximab–PHF–vinca at 1.4 mg/kg HPV equivalents.

approach takes advantage of the highly hydrophilic nature of the polymer, which can help to compensate for the increased hydrophobicity associated with higher DARs, thereby potentially improving the physicochemical and pharmacokinetic properties of the ADC. Indeed, the plasma PK of trastuzumab–PHF–vinca after a single administration to NCI-N87 tumor-bearing mice supports this hypothesis. As shown in Fig. 5A, trastuzumab–PHF–vinca exhibits a favorable plasma PK profile, with terminal elimination half-lives of approximately 9 and 3.5 days for total trastuzumab and conjugated HPV, respectively. Furthermore, free HPV, which could potentially contribute to systemic toxicity, was undetectable. As anticipated, administration of PHF–vinca without the benefit of antibody conjugation results in a rapid clearance, presumably via renal filtration of this relatively small, highly hydrophilic molecule.

Trastuzumab–PHF–vinca also exhibited robust, dose-dependent efficacy in the BT-474 breast cancer xenograft model, where dosing regimens of either 20 mg/kg once daily × 1 or 7.5 mg/kg once a week × 3 resulted in the maximum possible TGD and 100% tumor-free survivors at day 60 (Fig. 3). In this experiment, treatment with trastuzumab alone was inactive, and not surprisingly, when trastuzumab was coadministered with PHF–vinca, the combination of these two agents without the benefit of covalent conjugation resulted in only very modest activity. To further support that the efficacy of trastuzumab–PHF–vinca is due to antigen-dependent tumor accumulation, the non-binding ADC rituximab–PHF–vinca was also evaluated and resulted in a modest TGI, with no partial or complete regressions.

In a second BT-474 xenograft study, the activity of trastuzumab–PHF–vinca was confirmed at even lower doses; dosing regimens of 3.5 mg/kg once a week × 3 or 10 mg/kg once × 1 resulted in 10 of 10 tumor-free survivors on the final day of the study (day 87; Fig. 4). To assess the effect of tumor burden, treatment in one group of animals was delayed until average tumor volumes reached 344 mm^3. Despite the significantly increased initial tumor burden, trastuzumab–PHF–vinca was highly efficacious, exhibiting a 100% regression rate, with all animals confirmed tumor free by histopathology at the end of the study.

The time-course study comparing total HPV drug accumulation in tumors after administration of either the antigen-binding ADC trastuzumab–PHF–vinca or the non-binding ADC rituximab–PHF–vinca further substantiates the benefit of antigen-dependent tumor targeting (Fig. 5B). Consistent with Her2 antigen targeting, trastuzumab–PHF–vinca yielded a 4-fold greater C_{max} and 9-fold greater $AUC_{0\text{-}t}$ for total HPV in tumors relative to the non-binding ADC.

In summary, our polymer-based approach to ADCs offers a highly differentiated alternative to the conjugation platforms used in the ADCs that are currently in clinical development. The ability to achieve higher DARs without compromising drug-like properties, and thereby produce highly efficacious ADCs using moderately potent drug payloads provides a potential opportunity to expand the scope and utility of ADCs for the treatment of cancer.

Disclosure of Potential Conflicts of Interest

No potential conflicts of interest were disclosed.

Authors' Contributions

Conception and design: A.V. Yurkovetskiy, M. Yin, N. Bodyak, B. Zhu, T.B. Lowinger

Development of methodology: A.V. Yurkovetskiy, M. Yin, N. Bodyak, C.A. Stevenson, J.D. Thomas, B. Zhu, D.R. Gumerov, T.B. Lowinger

Acquisition of data (provided animals, acquired and managed patients, provided facilities, etc.): A.V. Yurkovetskiy, N. Bodyak, L.L. Qin, B. Zhu, D.R. Gumerov, E. Ter-Ovanesyan

Analysis and interpretation of data (e.g., statistical analysis, biostatistics, computational analysis): A.V. Yurkovetskiy, M. Yin, N. Bodyak, L.L. Qin, B. Zhu, T.B. Lowinger

Writing, review, and/or revision of the manuscript: A.V. Yurkovetskiy, M. Yin, N. Bodyak, D.R. Gumerov, T.B. Lowinger

Administrative, technical, or material support (i.e., reporting or organizing data, constructing databases): N. Bodyak, C.E. Hammond, L.L. Qin, B. Zhu, A. Uttard

Study supervision: A.V. Yurkovetskiy, D.R. Gumerov

Acknowledgments

The authors would like to acknowledge the contribution of Charles River Laboratories for conducting the *in vivo* studies and Xtal BioStructures for

conducting SPR experiments. The authors also express their gratitude to Drs. Donald Bergstrom, Radha Iyengar, and Peter U. Park for helpful comments on the article. Also, the significant assistance of Dr. Theresa E. Singleton in the preparation and editing of this manuscript is gratefully acknowledged.

The costs of publication of this article were defrayed in part by the payment of page charges. This article must therefore be hereby marked *advertisement* in accordance with 18 U.S.C. Section 1734 solely to indicate this fact.

Received January 13, 2015; revised May 15, 2015; accepted May 19, 2015; published OnlineFirst June 25, 2015.

References

1. Sievers EL, Senter PD. Antibody–drug conjugates in cancer therapy. Annu Rev Med 2013;64:15–29.
2. Deng C, Pan B, O'Connor OA. Brentuximab vedotin. Clin Cancer Res 2013;19:22–7.
3. Dieras V, Bachelot T. The success story of trastuzumab emtansine, a targeted therapy in HER2-positive breast cancer. Target Oncol 2014; 9:111–22.
4. Trail P. Antibody–drug conjugates as cancer therapeutics. Antibodies 2013;2:113–29.
5. Apelgren LD, Zimmerman DL, Briggs SL, Bumol TF. Antitumor activity of the monoclonal antibody-Vinca alkaloid immunoconjugate LY203725 (KS1/4-4-desacetylvinblastine-3-carboxhydrazide) in a nude mouse model of human ovarian cancer. Cancer Res 1990;50:3540–4.
6. Trail PA, Willner D, Lasch SJ, Henderson AJ, Hofstead S, Casazza AM, et al. Cure of xenografted human carcinomas by BR96-doxorubicin immunoconjugates. Science 1993;261:212–5.
7. Elias DJ, Hirschowitz L, Kline LE, Kroener JF, Dillman RO, Walker LE, et al. Phase I clinical comparative study of monoclonal antibody KS1/4 and KS1/4-methotrexate immunconjugate in patients with non–small cell lung carcinoma. Cancer Res 1990;50:4154–9.
8. Chari RV, Martell BA, Gross JL, Cook SB, Shah SA, Blattler WA, et al. Immunoconjugates containing novel maytansinoids: promising anticancer drugs. Cancer Res 1992;52:127–31.
9. Hamblett KJ, Senter PD, Chace DF, Sun MM, Lenox J, Cerveny CG, et al. Effects of drug loading on the antitumor activity of a monoclonal antibody–drug conjugate. Clin Cancer Res 2004;10:7063–70.
10. McDonagh CF, Turcott E, Westendorf L, Webster JB, Alley SC, Kim K, et al. Engineered antibody–drug conjugates with defined sites and stoichiometries of drug attachment. Protein Eng Des Sel 2006;19: 299–307.
11. Liu C, Tadayoni BM, Bourret LA, Mattocks KM, Derr SM, Widdison WC, et al. Eradication of large colon tumor xenografts by targeted delivery of maytansinoids. Proc Natl Acad Sci U S A 1996;93: 8618–23.
12. King HD, Dubowchik GM, Mastalerz H, Willner D, Hofstead SJ, Firestone RA, et al. Monoclonal antibody conjugates of doxorubicin prepared with branched peptide linkers: inhibition of aggregation by methoxytriethyleneglycol chains. J Med Chem 2002;45:4336–43.
13. Erickson HK, Lewis Phillips GD, Leipold DD, Provenzano CA, Mai E, Johnson HA, et al. The effect of different linkers on target cell catabolism and pharmacokinetics/pharmacodynamics of trastuzumab maytansinoid conjugates. Mol Cancer Ther 2012;11:1133–42.
14. Yurkovetskiy A, Choi S, Hiller A, Yin M, McCusker C, Syed S, et al. Fully degradable hydrophilic polyals for protein modification. Biomacromolecules 2005;6:2648–58.
15. Rooseboom M, Commandeur JN, Vermeulen NP. Enzyme-catalyzed activation of anticancer prodrugs. Pharmacol Rev 2004;56:53–102.
16. Conrad RA, Cullinan GJ, Gerzon K, Poore GA. Structure-activity relationships of dimeric Catharanthus alkaloids. 2. Experimental antitumor activities of N-substituted deacetylvinblastine amide (vindesine) sulfates. J Med Chem 1979;22:391–400.
17. Yurkovetskiy A, Yin M, Lowinger TB, Thomas JD, Hammond CE, Stevenson CA, et al., Inventors; protein–polymer–drug conjugates. US patent US 2012/0321583 A1. 2012.
18. Yurkovetskiy AV, Yin M, Lowinger TB, Thomas JD, Hammond CE, Stevenson CA, et al., Inventors; protein–polymer–drug conjugates. US patent US 2013/0101546 A1. 2013.
19. Walsh MD, Hanna SK, Sen J, Rawal S, Cabral CB, Yurkovetskiy AV, et al. Pharmacokinetics and antitumor efficacy of XMT-1001, a novel, polymeric topoisomerase I inhibitor, in mice bearing HT-29 human colon carcinoma xenografts. Clin Cancer Res 2012;18:2591–602.
20. Barok M, Tanner M, Koninki K, Isola J. Trastuzumab-DM1 is highly effective in preclinical models of HER2-positive gastric cancer. Cancer Lett 2011;306:171–9.
21. Govindan SV, Cardillo TM, Rossi EA, Trisal P, McBride WJ, Sharkey RM, et al. Improving the therapeutic index in cancer therapy by using antibody–drug conjugates designed with a moderately cytotoxic drug. Mol Pharm 2015;12:1836–47.

Cancer Research
The Journal of Cancer Research (1916–1930) | The American Journal of Cancer (1931–1940)

AACR American Association for Cancer Research

A Polymer-Based Antibody–Vinca Drug Conjugate Platform: Characterization and Preclinical Efficacy

Alexander V. Yurkovetskiy, Mao Yin, Natalya Bodyak, et al.

Cancer Res Published OnlineFirst June 25, 2015.